High Frequency Faradaic Rectification Voltammetry at Microelectrodes

Andrzej S. Baranski* and Piotr M. Diakowski

Department of Chemistry, University of Saskatchewan, 110 Science Place, Saskatoon, SK, Canada, S7N 5C9

Received: November 3, 2005; In Final Form: February 7, 2006

An experimental setup for carrying out faradaic rectification measurements at micrometer-sized electrodes under potential control is described. A new method of data analysis is proposed that allows the determination of the standard rate constant and the electron-transfer coefficient of a fast charge transfer process without knowing the impedance of the microelectrode. This method is based on the frequency dependence of the shape of the faradaic rectification voltammograms (i.e., the average width of the peaks and the ratio of the peak heights) rather than on the magnitude of the faradaic rectification signal. The method was tested in the determination of heterogeneous electron transfer kinetics of $Fe(CN)_6^{3-/4-}$ and $Ru(NH_3)_6^{2+/3+}$ in aqueous solutions on a platinum microelectrode (12.5 μm in radius) and ferrocene/ferrocinum redox couple in a dimethylformamide solution on a gold microelectrode (12.5 μm in radius).

Introduction

Faradaic rectification (FR) is a second-order impedance technique introduced by Doss and Agarwal[1] over 50 years ago. The major contributions to the development of that technique were made (among others) by Oldham[2], Barker,[3,4] Delahay,[5] and Sluyters-Rehbach and Sluyters.[6,7] Faradaic rectification originates from a nonlinear relationship between the electrical current passing through the electrode and the electrical potential that appears across the electrode interface; this nonlinearity also gives rise to higher harmonic components in the electrode response.

The technique is relatively simple from an experimental point of view; in the most common approach, an alternating (sinusoidal) current is applied to an electrode that is at equilibrium with a redox couple present in solution. However, because of the intrinsic nonlinearity of the system, the resulting polarization of the electrode is not sinusoidal and oscillations of the electrode potential are not symmetrically distributed about the equilibrium potential. As a consequence, the average electrode potential is different from the equilibrium potential; it depends on the amplitude of the alternating current, and, in a complex way, on the kinetics of the electrode reaction driven by that current. With conventionally sized electrodes, FR measurements at frequencies up to a few MHz are possible. That allows studies of kinetics of very fast charge transfer processes with the standard rate constant >1 cm/s. The limit in the use of high frequencies usually arises from the overheating of the solution (because at the higher frequencies, higher ac currents have to be used to create a measurable polarization of the electrode/solution interface). The electrode response is usually obtained by tracking changes in the average electrode potential caused by a low-frequency modulation of the alternating current passing through the cell.

It is also possible to do FR measurements differently, by controlling the electrode dc potential via an external electronic circuit and measuring the average FR current resulting from a sinusoidal polarization of the electrode. That technique was introduced by Barker[4] and it was called radio frequency polarography (some details will be provided in the next section of this paper). The FR techniques were relatively popular in the 50s and 60s, but later they were almost forgotten. The flame was kept alive by Agarwal, who published a couple of reviews on that topic.[8,9] Faradaic rectification was also discussed in a very useful review of ac techniques by Sluyters-Rehbach and Sluyters.[10] Furthermore, fundamentals of the FR methods are presented by Galus.[11] After 1990 only few papers related to fraradaic rectification appeared in the literature; the most interesting contributions dealt with an application of FR to the study of corrosion,[12] and with an abnormal distribution of electrical noise associated with electrode processes, which can be related to fraradaic rectification effects.[13]

It is not clear why researchers lost interest in the development and applications of FR techniques − perhaps this technique was introduced too early. Although faradaic rectification measurements are easy to carry out, results are difficult to interpret and data processing is very laborious. In fact, it is hard to imagine how collection and analysis of data could be done without extensive use of computers which, of course, were much less powerful, less user-friendly, and not easily accessible when the technique was developed. In a general sense (at least from a mathematical perspective), faradaic rectification is very similar to the optical second harmonic generation (SHG) technique. The latter was introduced[14] nine years after the former, but today SGH is used by thousands of researchers around the world.

We believe that FR techniques can be extremely valuable in modern electrochemical research. In addition to experimental simplicity, FR techniques have another very strong advantage over conventional techniques: they allow the measurement of very fast electrode kinetics. The speed of conventional techniques is limited by the electrode time constant, expressed as a product of the double layer capacitance, C_{dl}, and the solution resistance, R_s. For example, in conventional ac impedance measurements, frequency cannot be much larger than $1/C_{dl}R_s$ because in such a situation the electrode impedance would approach R_s and accurate determination of the electrode kinetics would become impossible. A similar limitation exists in cyclic voltammetry. If the scan rate is much larger than $RT/nFC_{dl}R_s$, the cyclic voltammogram is highly distorted and again the

* Corresponding author. E-mail: baranski@duke.usask.ca

10.1021/jp056352f CCC: $33.50
Published on Web 03/09/2006

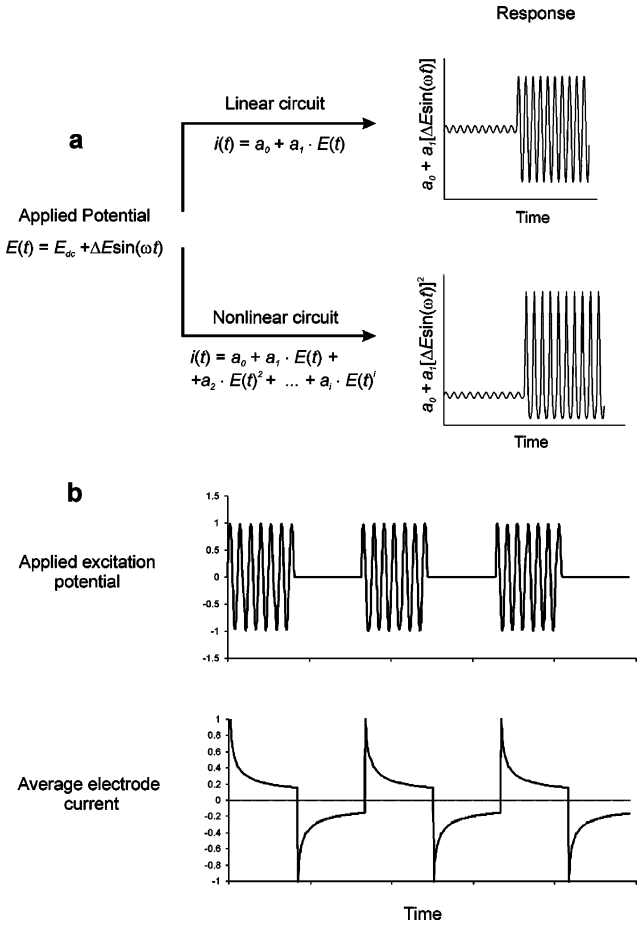

Figure 1. (a) Response of a linear and a nonlinear system to a sinusoidal excitation waveform. (b) Excitation waveform and a current response in faradaic rectification voltammetry.

determination of kinetic parameters of the electrode reaction is unattainable. FR techniques are not restrained by the electrode time constant because solution resistance and (to some extent) double layer capacitance are linear elements, and they do not generate FR signals. Consequently, measurements can be carried out in a frequency range that is not accessible to conventional ac impedance methods.

In this paper we describe a study of faradaic rectification under voltammetric conditions at platinum and gold microelectrodes. Measurements are performed in a way similar to the one proposed by Barker;[4] however, to obtain kinetic results, we developed a different method of data analysis that is based on the shape of FR curves rather than on their magnitude. Consequently, we can determine the kinetic parameters of a fast charge transfer process (the standard rate constant and the electron transfer coefficient) without knowing the impedance of the microelectrode.

Principles of Faradaic Rectification Voltammetry

The idea of faradaic rectification under controlled potential conditions is presented in Figure 1. First let us consider a voltage waveform described as: $E_{dc} + \Delta E\sin(\omega t)$ (where: E_{dc} is a constant component, whereas ΔE and ω are the amplitude and the angular frequency of the alternating component) applied to a linear element of an electrical circuit (such as a resistor, R, or a capacitor, C). The current flowing through that element is proportional to the applied voltage and, in general, is expressed as $a_0 + a_1 \cdot \Delta E\sin(\omega t + \varphi)$. In the case of resistor $a_0 = E_{dc}/R$, $a_1 = 1/R$, $\varphi = 0$, and in the case of capacitor $a_0 = 0$, $a_1 = \omega/R$ and $\varphi = -\pi/2$, the current averaged within the one oscillation period ($T = 2\pi/\omega$) is independent of the amplitude (ΔE) because the average value of the $\sin(\omega t + \varphi)$ function within one period is zero. Now, if the same voltage waveform is applied to a nonlinear element (such as a diode in a forward bias or an electrode at which an electrochemical reaction is taking place), the resulting current is a nonlinear function of the applied voltage, which can be represented as a Taylor series:

$$i(t) = a_0 + a_1\Delta E\sin(\omega t + \varphi_1) + a_2[\Delta E\sin(\omega t + \varphi_2)]^2 + a_3[\Delta E\sin(\omega t + \varphi_3)]^3 + \ldots \quad (1)$$

It should be noted that the average value of the $[\sin(\omega t + \varphi_n)]^k$ function within one period is greater than 0 if k is even, or equal to 0 if k is odd. Therefore, in general, the current passing through nonlinear elements depends on ΔE, because of the contribution from even components of eq 1. Nonlinear elements also generate higher harmonics in the response, because the $[\sin(\omega t + \varphi_n)]^k$ function can be represented as sum of even harmonics from 0 to k (if k is even), or odd harmonics from 1 to k (if k is odd).

In electrochemical measurements, the amplitude of the alternating voltage is usually modulated by a square wave function. Normally, the alternating voltage is simply switched "on" and "off" at the beginning of subsequent half-cycles of the square wave function, as shown in Figure 1b. The modulation frequency is more than 100 times smaller than the alternating voltage frequency. The resulting current passes through a low-pass filter that completely removes oscillations caused by the alternating voltage. Therefore, the measured current, $\bar{\imath}_m$, is effectively the same as the current averaged within the $2\pi/\omega$ period, and shows only averaged contributions from even components of eq 1:

$$\bar{\imath}_m = a_0 + \frac{a_2}{2}\Delta E^2 + \frac{3a_4}{8}\Delta E^4 + \ldots \quad (2)$$

Of course, that current drives an electrochemical reaction at the electrode solution interface. For example, $\bar{\imath}_m > 0$ drives an oxidation reaction that causes a depletion of the reduced form (Red) and a build up of the oxidized form (Ox) of the redox couple at the electrode; as a result, $\bar{\imath}_m$ decays with time within the modulation half-period. The modulation current can be recorded by instruments (such as data acquisition cards) having a relatively low bandwidth (a bandwidth roughly 4 times larger than the modulation frequency is sufficient). Normally, the difference between currents observed at the ends of the subsequent half-cycles is determined and plotted as a function of E_{dc}; that difference is called the faradaic rectification current, Δi_{FR}.

$$\Delta i_{FR} = \bar{\imath}_m^{on} - \bar{\imath}_m^{off} \quad (3)$$

Note that in the FR current, the zeroth harmonic component (a_0) is normally canceled out.

Barker[4] derived an asymptotic equation (valid for $\Delta E \ll RT/nF$) which describes the shape of a functional relationship between Δi_{FR} and E_{dc} in the case of electrode processes involving Red and Ox species dissolved in solution:

$$\Delta i_{FR} = \kappa\left[\frac{(1-2\alpha)P^{2\alpha}\chi^2 + \sqrt{2}P^{\alpha}(1-\alpha-\alpha P)\chi + 1 - P^2}{P^{2\alpha}\chi^2 + \sqrt{2}P^{\alpha}(1+P)\chi + (1+P)^2}\right]\frac{P}{(1+P)^2}\Delta E^2 \quad (4)$$

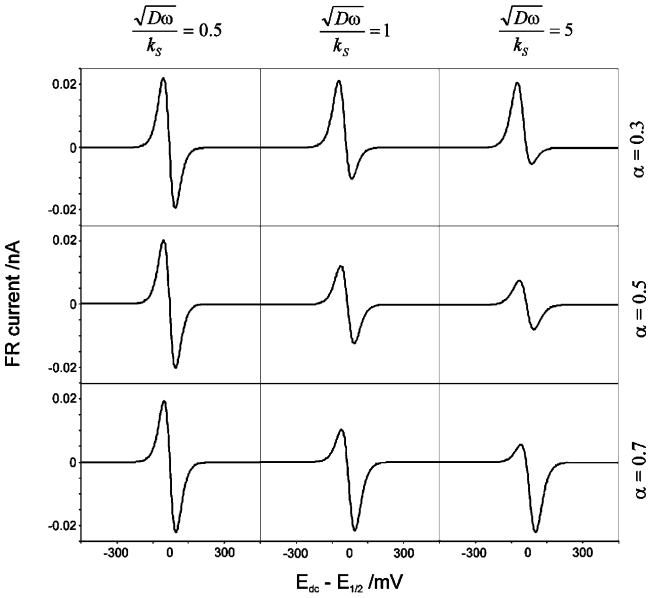

Figure 2. Faradaic rectification voltammograms predicted by eq 4 for different values of α and $\chi = (\sqrt{D\omega})/k_s$.

with

$$P = \exp\left[(E_{dc} - E_{1/2})\frac{nF}{RT}\right] \quad (5)$$

and

$$\chi = \frac{\sqrt{\omega D}}{k_s} \quad (6)$$

In these equations, κ is a coefficient proportional to the reactant concentration and the electrode surface area and dependent also on the modulation frequency and the current sampling procedure, α is the electron transfer coefficient, k_s is the standard rate constant of the electrode reaction, ω is the angular frequency of the alternating voltage, D is the diffusion coefficient of the redox species, $E_{1/2}$ is the half-wave potential, n is the number of electrons transferred during the redox process per molecule of the reactant, and other symbols have their normal meaning.

Equation 4 is valid for processes that are reversible at the modulation frequency, but they can be reversible or irreversible at the alternating voltage frequency.

The shapes of FR curves predicted by eq 4 for different values of α and χ parameters are shown in Figure 2. For $\chi \ll 1$ the electrode process is completely reversible at the alternating voltage frequency; consequently, FR curves are independent of α. They contain two peaks: a positive one (M_{max}) that occurs at potential more negative than the half-wave potential ($E_{max} < E_{1/2}$) and a negative one (M_{min}) that occurs at $E_{min} > E_{1/2}$. The heights of these peaks are the same in magnitude and opposite in sign, so the ratio parameter defined by eq 7 is equal to 1.

$$R_{FR} = \left(-\frac{M_{max}}{M_{min}}\right)_{-M_{min} \geq M_{max}} \text{ or } R_{FR} = \left(-\frac{M_{min}}{M_{max}}\right)_{M_{max} > -M_{min}} \quad (7)$$

As ω increases, χ becomes larger and the magnitude of the faradaic rectification peaks changes. Figure 3 shows normalized values $\Delta\tilde{M}_{FR} = (M_{max} - M_{min})/\Delta E^2$ plotted as a function of $\log(\chi)$ for different values of α. Numbers attached to the curves represent $0.5 - |0.5 - \alpha|$; they are equal to α, for $\alpha \leq 0.5$, and

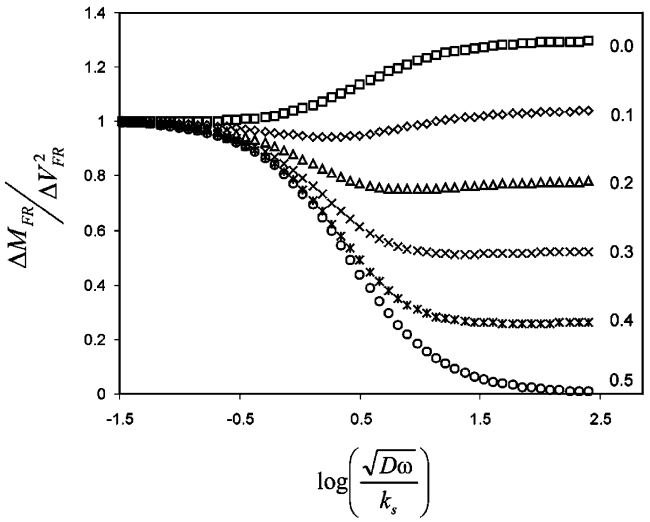

Figure 3. Normalized magnitude of faradaic rectification peaks shown as a function of $\chi = (\sqrt{D\omega})/k_s$. Numbers attached to the curves represent $0.5 - |0.5 - \alpha|$.

$1 - \alpha$, for $\alpha > 0.5$. This means that, for example, that the curves for $\alpha = 0.3$ and $\alpha = 0.7$ are identical. When $\alpha = 0.5$: $\Delta\tilde{M}_{FR} \rightarrow 0$ as $\chi \rightarrow \infty$, but in other cases, $\Delta\tilde{M}_{FR}$ reaches a finite value as $\chi \rightarrow \infty$. If $\alpha < 0.12$ or $\alpha > 0.88$ then $\Delta\tilde{M}_{FR}$ for a totally irreversible process (i.e., for $\chi \rightarrow \infty$) is larger than $\Delta\tilde{M}_{FR}$ for a completely reversible process (i.e., for $\chi \rightarrow 0$), and in other cases $(\Delta\tilde{M}_{FR})_{\chi\rightarrow\infty} < (\Delta\tilde{M}_{FR})_{\chi\rightarrow 0}$.

When $\alpha = 0.5$, the R_{FR} defined by eq 7 is always equal to 1, regardless of the χ parameter; however, for $\alpha \neq 0.5$: R_{FR} decreases to zero as χ approaches infinity. The relationship between R_{FR} and χ is the same for the same value of $0.5 - |0.5 - \alpha|$. It should be noted, however, that for $\alpha < 0.5$, M_{min} decreases faster than M_{max} with an increase of χ, and for $\alpha > 0.5$ the trend is the opposite. Therefore, $M_{max} > -M_{min}$ indicates $\alpha < 0.5$ and $M_{max} < -M_{min}$ indicates $\alpha > 0.5$.

Experimental Section

Reagents. All aqueous solutions were prepared in double-distilled deionized water (Corning Mega-Pure System, MP-6A and D-2). In some measurements, glass distilled *N*,*N*-dimethylformamide (DMF) from EM Science was used. $Ru(NH_3)_6Cl_3$ was purchased from Alfa Aesar and Ferrocene from Aldrich Chemical Co. Inc.; all other chemicals were ACS grade. All electrochemical measurements were carried out in a standard electrochemical cell with an Ag|AgCl|(sat'd) KCl reference electrode and a platinum auxiliary electrode (about 1 cm^2 in the surface area). Dissolved oxygen was not removed from the solutions, because oxygen reduction did not interfere with the studied processes. Three redox systems were studied: $Fe(CN)_6^{3-/4-}$ in an aqueous solution of 5 M KOH and 0.1 M KCN, ferrocene/ferrocinum, in a DMF solution of 0.2 M $KClO_4$, and $Ru(NH_3)_6^{2+/3+}$ in an aqueous solution of 3.5 M NH_4Cl and 1.5 M NH_3.

Working electrodes were prepared by sealing Pt or Au wires (Alfa Aesar, A Johnson Matthey Company) into Corning Kovar Sealing glass tubing #7052 (World Precision Instruments). A lead was made by connecting copper wire with microwires with the aid of silver conductive adhesive paste (Alfa Aesar). The surface of the working electrode was polished with aluminum oxide finishing films (TrueView Products Inc.). Initial polishing was done with 3 μm aluminum oxide, and the final mirror-like

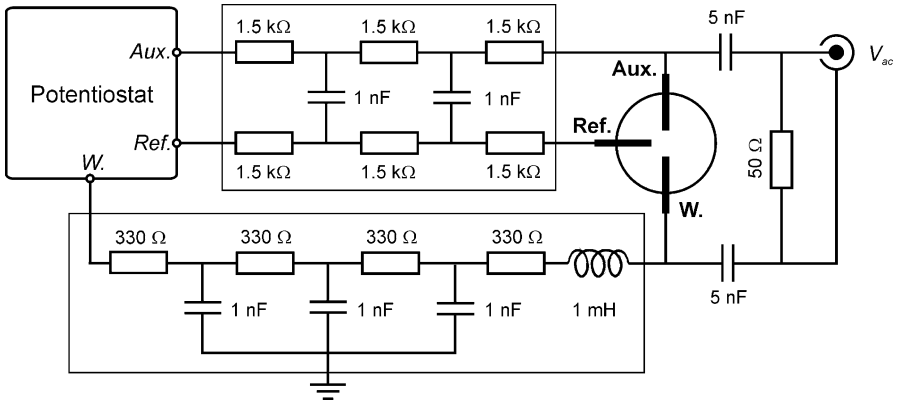

Figure 4. Experimental setup used in faradaic rectification voltammetry.

polish was obtained with a 0.3 μm aluminum oxide. The size of all disk electrodes used in this work is described in terms of their radius.

Electronic Circuit. The diagram of the electronic setup used in this work is shown in Figure 4. The high-frequency sinusoidal waveform was produced by a Hewlett-Packard signal generator (model HP8648B). This generator could produce a signal with frequency ranging from 10 kHz to 2 GHz and voltage amplitude up to 2.6 V_{rms} (that limit actually varied somewhat with frequency). In this work only frequencies between 100 kHz and 12.5 MHz were used, and the amplitude was no larger than 500 mV rms. The waveform (later called the excitation signal) was applied to an AC input of the potentiostat marked as V_{ac} in Figure 4. The connection between the HP8648B and the potentiostat was made with a short (~60 cm) coaxial cable terminated with a 50 Ω resistor. The main pathway for the excitation signal was from input V_{ac} to a 5 nF capacitor, the auxiliary electrode, the solution, the working microelectrode, and through another 5 nF capacitor to ground. Other pathways were limited by filters F1 and F2. All capacitors shown in this diagram were low inductance mica capacitors. Since in the studied frequency range the impedance of 5 nF capacitors was relatively small, the ac potential drop at these capacitors was negligible. Furthermore, the auxiliary electrode/solution interface was practically not polarized by the alternating voltage (because the interfacial capacitance was very large), and, therefore, the alternating potential difference that developed between the working microelectrode and the bulk solution was practically the same as that applied to the AC input of the potentiostat. Currents passing between Aux and W terminals of the potentiostat were very small (<50 nA), so resistors present in filters F1 and F2 did not produce any measurable ohmic drop. It should be stressed that the use of these filters is absolutely necessary, because otherwise relatively large alternating currents passing through the cell could overload the potentiostat. The potentiostat used in this work was based on a classical design[15] with the working electrode held at virtual ground potential. The bandwidth of the potentiostat was between 10 kHz and 1 kHz (depending on the current range) and the lowest current range was 0.05 nA per full scale.

Measurements were carried out with a custom designed data acquisition system based on a microcontroller (Microchip PIC18F452) which was interfaced with a computer via a serial link. The dc potential of the working electrode was controlled by a 16-bit digital-to-analog converter (Linear LTC1655). Scanning of the dc potential range was performed in a staircase fashion. The potential steps in the scanning waveform were always less than 10 mV, and the scanning rate was typically less than a 0.01 V/s. The current was sampled with a 16-bit analog-to-digital converter (Texas Instruments TLC4545) after passing through an anti-aliasing filter made of a clock-tunable fifth-order Bessel low pass filter (Linear LTC1065). The system was also equipped with a 12-bit digital-to-analog converter which was used to modulate the output of the HP8648B generator (by changing the ac amplitude from a desired value to zero in a square wave fashion). The modulation frequency was typically 100 Hz. The response current was sampled at least 100 times during each modulation cycle, and then the average values of current were calculated within four quarters of the modulation cycle (the first two quarters corresponded to the alternating voltage turned "on" and the subsequent two quarters corresponded to the alternating voltage turned "off"). The FR current at a given dc potential was calculated as a difference between the mean current in the second quarter minus the mean current in the fourth quarter of the modulation cycle. Typically, 32 modulation cycles were performed at each dc potential and the values of the FR current obtained at the same dc potential were averaged. The averaged FR current was displayed as a function of the dc potential and stored on a computer disk for future analysis. Simultaneously with each FR voltammogram, we also recorded the average dc current as a function of the dc potential (that information allows the detection of possible heating of the electrode).

The software for the microcontroller was written in assembly language (with an assembler provided by Microchip) and the PC software (for data acquisition and processing) was written using Microsoft Visual C++, version 6.0 and Visual Basic, version 6.0. The experimental data were further processed in Microsoft Excel. Visual Basic, version 6.0 was also used to write a computer program that generated FR voltammograms based on Barker's equation (eq 4) and to calculate quantities shown in Figures 2, 3, 6, 7, 8, 9, and 10 and in Table 1.

Results and Discussion

In Figure 5, FR voltammograms obtained at a 12.5 μm Pt microelectrode in an aqueous solution containing 5 M KOH, 0.1 M KCN, and 10 mM $K_4Fe(CN)_6$ are shown. The alternating voltage frequencies were 0.1, 0.34, and 3.8 MHz. As predicted by theory, with increasing frequencies the peaks get smaller and the absolute ratio of the negative to the positive peak decreases. Equation 4 can be used to analyze FR results obtained with a disk microelectrode, despite the fact that it was originally derived based on a description of the faradaic impedance applicable to linear diffusion. It has been previously shown[16] that nonlinear diffusion terms in the faradaic impedance of disk microelectrodes become negligible when $\omega \gg D/r_o^2$ (where r_0 is the radius of the disk electrode). In our case, $D/r_o^2 \approx 6.4$,

TABLE 1: Numerical Data Obtained from Analysis of Eq 4 Useful in the Determination of Kinetic Parameters from FR Voltammograms

			$nF\bar{W}^0_{FR}/RT$		
$0.5 - \lvert 0.5 - \alpha \rvert$	slope[a]	intercept[b]	$R^0_{FR} = 0.25$	$R^0_{FR} = 0.50$	$R^0_{FR} = 0.75$
0.000	-0.901 ± 0.001	-0.0065 ± 0.0002	2.82 ± 0.01	2.651 ± 0.005	2.6056 ± 0.0007
0.100	-0.849 ± 0.003	0.0955 ± 0.0006	2.87 ± 0.01	2.686 ± 0.005	2.6217 ± 0.0007
0.200	-0.794 ± 0.004	0.213 ± 0.001	2.96 ± 0.01	2.748 ± 0.005	2.6538 ± 0.0008
0.250	-0.764 ± 0.005	0.282 ± 0.001	3.01 ± 0.01	2.795 ± 0.005	2.6786 ± 0.0007
0.300	-0.727 ± 0.005	0.364 ± 0.001	3.08 ± 0.01	2.856 ± 0.004	2.7131 ± 0.0005
0.350	-0.687 ± 0.005	0.466 ± 0.001	3.18 ± 0.01	2.939 ± 0.003	2.7636 ± 0.0001
0.400	-0.672 ± 0.006	0.605 ± 0.001	3.308 ± 0.008	3.063 ± 0.001	2.847 ± 0.001
0.425	-0.666 ± 0.006	0.704 ± 0.001	3.398 ± 0.006	3.154 ± 0.001	2.913 ± 0.003
0.450	-0.656 ± 0.006	0.845 ± 0.001	3.518 ± 0.003	3.283 ± 0.003	3.019 ± 0.005
0.475	-0.667 ± 0.006	1.095 ± 0.001	3.692 ± 0.0005	3.496 ± 0.007	3.22 ± 0.01
0.495	-0.882 ± 0.006	1.885 ± 0.001	3.918 ± 0.001	3.842 ± 0.006	3.68 ± 0.01
0.499	-0.813 ± 0.008	2.410 ± 0.003	3.95 ± 0.01	3.95 ± 0.01	3.91 ± 0.03

[a] The slope of $\log(\chi)$ vs $\log[(R^0_{FR})/(1 - R^0_{FR})]$ plot at $R^0_{FR} = 0.5$. [b] The intercept of $\log(\chi)$ vs $\log[(R^0_{FR})/(1 - R^0_{FR})]$ plot.

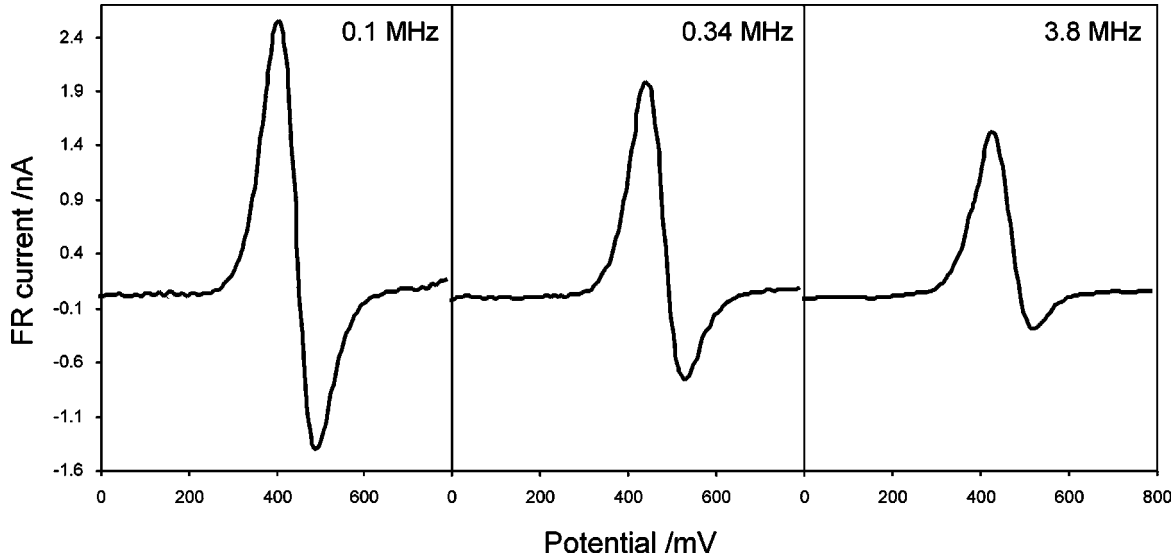

Figure 5. Faradaic rectification voltammograms obtained at a 12.5 μm Pt microelectrode in an aqueous solution containing 5 M KOH, 0.1 M KCN, and 10 mM $K_4Fe(CN)_6$. Alternating voltage amplitudes were: 40 mV_{rms} for 0.1 and 0.34 MHz and 160 mV_{rms} for 3.8 MHz.

therefore the condition is fulfilled for the excitation frequencies ($\omega \geq 6.28 \times 10^5\ s^{-1}$) and for the modulation frequency ($\omega \approx 628\ s^{-1}$).

Barker proposed a method for the determination of kinetic parameters based on measurements of $\Delta M_{FR} = M_{max} - M_{min}$ and R_{FR} for a given electrochemical system at two different alternating voltage frequencies (for example 100 kHz and 1.6 MHz). However, eq 4 shows that ΔM_{FR} is proportional to ΔE^2, and experiments show that R_{FR} also depends somewhat on ΔE^2. Therefore, this method works only if the measurements at different frequencies are made using the same ΔE. That creates a problem; we can easily control the alternating voltage applied to the electrode, ΔV_{ac}, (or the alternating current passing through the cell, ΔI_{ac}, as it was in Barker's measurements), but in order to calculate the alternating voltage that appears across the working electrode interface we need to know the electrode impedance.

Based on the Randles equivalent circuit:[17]

$$\Delta E = \Delta V_{ac}\left|\frac{Z_{if}}{Z_{if} + R_s}\right| \tag{8}$$

or

$$\Delta E = \Delta I_{ac}|Z_{if}| \tag{9}$$

where Z_{if} is the impedance of the electrode interface and R_s is the solution resistance.

$$Z_{if} = \frac{1}{1/Z_{dl} + 1/Z_F} \tag{10}$$

where Z_{dl} is the reactance of double layer capacitance and Z_F is the impedance of the electrode reaction.

When concentration of species participating in the electrode reaction is low and the alternating voltage frequency is high, then $|Z_F| \gg |Z_{dl}|$ and $Z_{if} \approx Z_{dl}$. It should be noted that Z_{if}, Z_{dl}, and Z_F are complex numbers, so in eqs 8, 9, and 10 the rules of complex algebra should be followed.

Barker[4] carried out FR measurements using a dropping mercury electrode. The double layer capacitance of the mercury electrode is well known, and it does not show significant frequency dispersion (at least at low frequencies), so Z_{dl} can be calculated as

$$Z_{dl} = -\frac{j}{C_{dl}\omega} \tag{11}$$

where C_{dl} is the double layer capacitance, ω the angular frequency of the alternating voltage (or current), and $j = \sqrt{-1}$.

Unfortunately, the double layer capacitance of mercury electrodes shows some frequency dispersion at frequencies

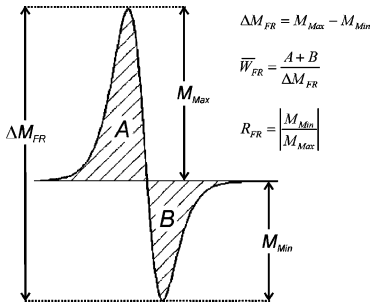

Figure 6. Determination of the average peak width ($\bar{W}_{FR}$) and the peak ratio parameter (R_{FR}).

greater than 1 MHz,[18] and the double layer capacitance of solid microelectrodes, in general, depends very strongly on frequency, consequently, eq 11 cannot be used; instead the double layer impedance is represented as a so-called constant phase element.[16,19] Consequently, the method of data analysis proposed by Barker[4] would not work at high frequencies (particularly at solid microelectrodes) and a new method of data analysis of FR results has to be developed.

In addition to ΔM_{FR} and R_{FR}, other characteristic parameters of the FR curves that depend on χ and α are the peak width and the peak separation ($E_{min} - E_{max}$). In general, both the peak width and the peak separation increase as χ increases. In the case of digital data acquisition and computer data analysis, a parameter particularly easy to determine is the average peak width defined as the ratio of the area under both peaks divided by $M_{max} - M_{min}$ (see also Figure 6):

$$\bar{W}_{FR} = (1/M_{max} - M_{min}) \int_{-\infty}^{+\infty} |i_{FR}(E_{dc})| \, dE_{dc} \qquad (12)$$

It is convenient to discus $\bar{W}_{FR}$ normalized by RT/nF since that normalization removes the dependence of $\bar{W}_{FR}$ on n and temperature.

Both $nF\bar{W}_{FR}/RT$ and R_{FR} depend somewhat on the amplitude of the alternating voltage (ΔE). That dependence is not shown in eq 4, but it can be observed experimentally and it is predicted by numerical simulations (which will be published in a separate paper). Experiments show that R_{FR} and $nF\bar{W}_{FR}/RT$ depend linearly on the square of the amplitude of the alternating voltage applied to the electrochemical cell (ΔV_{ac}^2) as it is shown in Figure 7. Consequently, experimental values of R_{FR} and $nF\bar{W}_{FR}/RT$ can be extrapolated to $\Delta V_{ac}^2 \rightarrow 0$, and these extrapolated values (referred to as R_{FR}^0 and $\bar{W}_{FR}^0$, respectively) can be analyzed in terms of eq 4. According to eq 8, at constant frequency the ratio of $\Delta E/\Delta V_{ac}$ is constant, therefore extrapolation to $\Delta V_{ac}^2 \rightarrow 0$ gives the same result as extrapolation to $\Delta E^2 \rightarrow 0$.

The theoretical relationship between $\log(\chi)$ and $\log[R_{FR}^0/(1 - R_{FR}^0)]$ for different values of α is shown in Figure 8 (numbers attached to the curves represent $0.5 - |0.5 - \alpha|$; they are equal to α, for $\alpha \leq 0.5$, and $1 - \alpha$, for $\alpha > 0.5$). If the range of $\log[R_{FR}^0/(1 - R_{FR}^0)]$ values is not too large (say, between -0.5 and 0.5), these plots are practically linear. The numerical values of the slopes and the intercepts of these plots, for different values of $0.5 - |0.5 - \alpha|$, are listed in Table 1. It should be noted that that the intercept increases rapidly as $\alpha \rightarrow 0.5$, and for $\alpha = 0.5$ the intercept is undefined, because in this case $R_{FR}^0 = 1$ for any value of χ.

The theoretical relationship between $(nF\bar{W}_{FR}^0)/RT$ and R_{FR}^0 for different values of $0.5 - |0.5 - \alpha|$ is shown in Figure 9. For $\alpha \neq 0.5$ when $R_{FR}^0 \rightarrow 1$, $(nF\bar{W}_{FR}^0)/RT \rightarrow 2.60$ and when $R_{FR}^0 \rightarrow 0$, $(nF\bar{W}_{FR}^0)/RT \rightarrow 3.96$. In Table 1, numerical values of $(nF\bar{W}_{FR}^0)/RT$ for R_{FR}^0 equal to 0.25, 0.50, and 0.75 are listed for different values of $0.5 - |0.5 - \alpha|$. A curve for $\alpha = 0.5$ is not shown in Figure 9, but it can be represented as a vertical line at $R_{FR}^0 = 1$. In this case, R_{FR}^0 is always the same but the average width of the peaks depends on χ. A plot of $(nF\bar{W}_{FR}^0)/RT$ versus $\log(\chi)$ for $\alpha = 0.5$ is shown in Figure 10. The normalized average width, $(nF\bar{W}_{FR}^0)/RT$, changes from 2.60 to 3.96 as χ increases, and it reaches the middle value of 3.28 when $\chi = 6.97$. Data in Figures 9 and 10 and in Table 1 were obtained by the numerical integration of eq 4.

One can use the data presented in Figures 8 and 9 to determine the kinetic parameters of an electrode process without knowing the electrode impedance (alternatively, when $\alpha = 0.5$, data presented in Figure 10 can be used).

To determine the kinetic parameters of the $Fe(CN)_6^{3-}/Fe(CN)_6^{4-}$ electrode reaction, we used FR curves recorded at various frequencies (from 0.1 to 3.8 MHz) and for different ΔV_{ac} amplitudes. The amplitudes were selected large enough to produce an FR response with a good signal-to-noise ratio

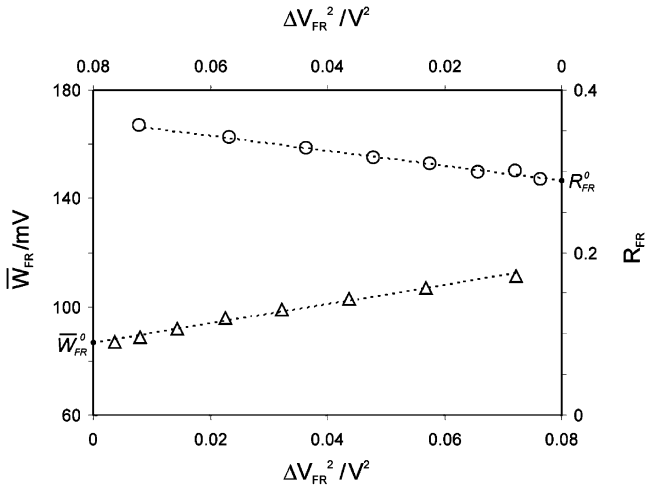

Figure 7. Effect of the alternating voltage amplitude on $\bar{W}$ and R_{FR}. Based on faradaic rectification voltammograms obtained at 1.14 MHz in an aqueous solution containing 5 M KOH, 0.1 M KCN, and 10 mM $K_4Fe(CN)_6$ at a 12.5 μm Pt microelectrode.

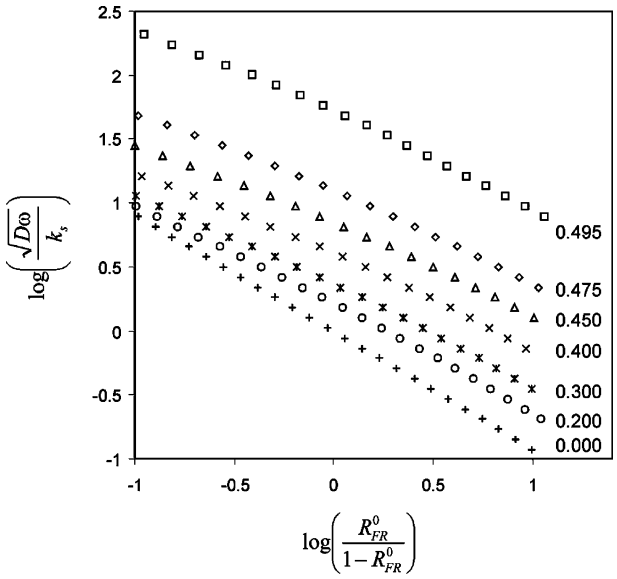

Figure 8. Relationship between $\log(\chi)$ and $\log[(R_{FR}^0)/(1 - R_{FR}^0)]$ predicted by eq 4. Numbers attached to the curves represent $0.5 - |0.5 - \alpha|$.

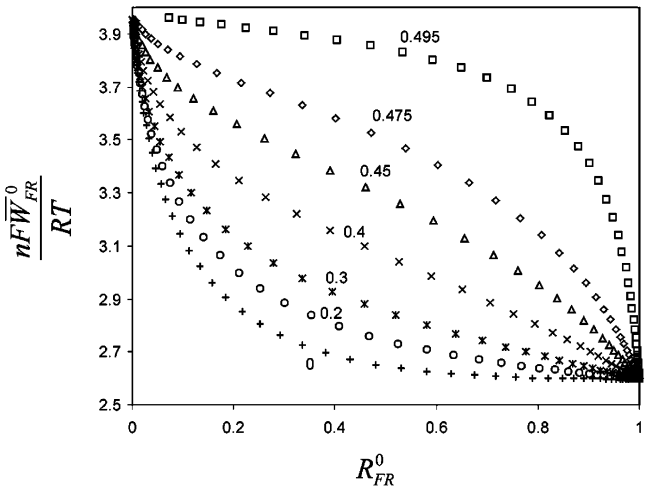

Figure 9. Relationship between $(nF\bar{W}^0_{FR})/RT$ and R^0_{FR} predicted by eq 4. Numbers attached to the curves represent $0.5 - |0.5 - \alpha|$.

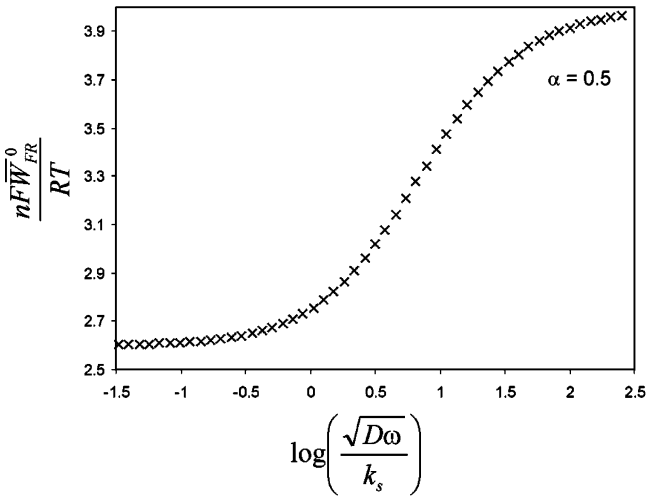

Figure 10. A relationship between $(nF\bar{W}^0_{FR})/RT$ and $\log(\chi)$ predicted by eq 4 for $\alpha = 0.5$.

(>100) but not too large, so plots of $\log(\Delta M_{FR})$ versus $\log(\Delta V_{ac})$ had slopes between 1.9 and 2.0 (a slope significantly lower than 2 indicates that the amplitude is too large). For each amplitude at a given frequency, $\bar{W}$ and R_{FR} were calculated and plotted versus ΔV^2_{ac}, then extrapolated values: $\bar{W}^0_{FR}$ and R^0_{FR} were obtained by the least-squares method. Next a plot of $(nF\bar{W}^0_{FR})/RT$ versus R^0_{FR} was made (as shown in Figure 11), and from that plot experimental values of $(nF\bar{W}^0_{FR})/RT$ for R^0_{FR} equal to 0.25 and 0.50 were determined by a third-order polynomial curve fitting (3.404 and 3.196, respectively).

These experimental values of normalized widths were used to determine the α coefficient, by comparing them with the theoretical values listed in Table 1. In this case, α must be smaller than 0.5, because the positive peak is larger than the negative peak (as shown in Figure 5). By using a linear interpolation method, we obtained $\alpha = 0.426$ (from the width at $R^0_{FR} = 0.25$) and $\alpha = 0.433$ (from the width at $R^0_{FR} = 0.50$).

Then we used the average value of α (0.430) to determine $\log(\chi_{R_{FR}{}^0=0.5})$ based on the numerical data listed in Table 1. The linear interpolation method yielded $\log(\chi_{R_{FR}{}^0=0.5}) = 0.72 \pm 0.02$ and $\chi_{R_{FR}{}^0=0.5} = 5.3 \pm 0.2$. Finally, a plot of $\log(\sqrt{D\omega})$ versus $\log[(R^0_{FR})/(1 - R^0_{FR})]$ for the experimental results was made (see Figure 12) and $\log(\sqrt{D\omega_{R_{FR}{}^0=0.5}})$ was determined from the intercept of that plot by the linear least-squares regression

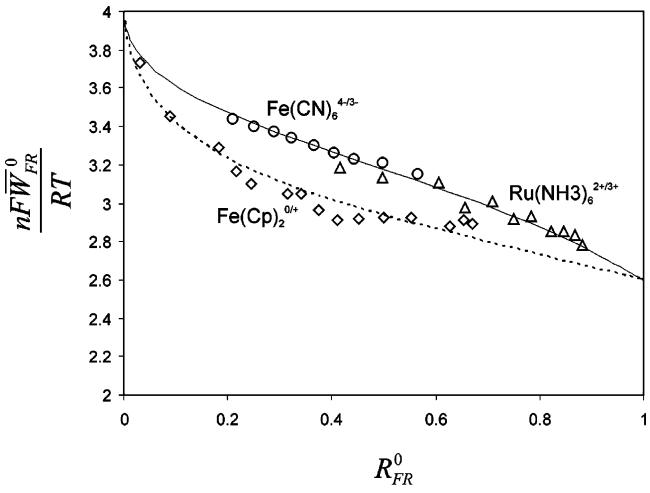

Figure 11. Relationship between $(nF\bar{W}^0_{FR})/RT$ and R^0_{FR} observed for three different redox systems: $Fe(CN)_6^{3-/4-}$ (○), $Ru(NH_3)_6^{2+/3+}$ (△), and $Fe(Cp)_2^{0/+}$ (◇). The solid curve represents a theoretical relationship for $\alpha = 0.43$ (or $\alpha = 0.57$), and the dashed curve represents a theoretical relationship for $\alpha = 0.35$ (or $\alpha = 0.65$).

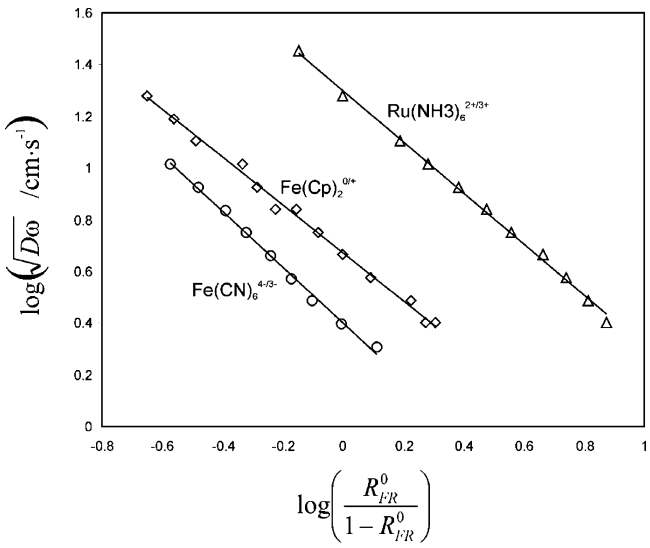

Figure 12. Relationship between $\log(\sqrt{D\omega})$ and $\log[(R^0_{FR})/(1 - R^0_{FR})]$ observed for three different redox systems: $Fe(CN)_6^{3-/4-}$ (○), $Ru(NH_3)_6^{2+/3+}$ (△), and $Fe(Cp)_2^{0/+}$ (◇).

method. That method yielded $\log(\sqrt{D\omega_{R_{FR}{}^0=0.5}}) = 0.402 \pm 0.009$ and $\sqrt{D\omega_{R_{FR}{}^0=0.5}} = 2.52 \pm 0.06$.

Since $\chi_{R_{FR}{}^0=0.5} = (\sqrt{D\omega_{R_{FR}{}^0=0.5}})/k_s$, the standard rate constant of the electron-transfer process can be calculated as

$$k_s = \frac{\sqrt{D\omega_{R_{FR}{}^0=0.5}}}{\chi_{R_{FR}{}^0=0.5}} \tag{13}$$

where the numerator is from the plot of experimental data and the denominator is from Table 1.

Equation 13 gives $k_s = 0.48 \pm 0.02$ cm/s. This value is in good agreement with the standard rate constant of 0.55 ± 0.07 cm/s obtained for the $Fe(CN)_6^{3-/4-}$ redox couple in 1 M KCl and 3 mM KCN by Huang and McCreery,[20] who used fast voltammetry at Pt microdisk electrodes. The authors noted that without the addition of cyanide, the standard rate constant of ferrocyanide decreases due to the blocking of the electrode by products of $Fe(CN)_6^{3-/4-}$ decomposition to a Prussian-blue-like film. That may explain why most authors who did not add CN−

TABLE 2: Kinetic Parameters of Electron Transfer Processes Studied with Faradaic Rectification Voltammetry

Redox system, electrode and the supporting electrolyte	diffusion coefficient[a] [cm^2s^{-1}]	electron transfer coefficient	standard rate constant [cm s^{-1}]
$Fe(CN)_6^{3-/4-}$, Pt, 5 M KOH, 0.1 M KCN in H_2O	6.6×10^{-6}	0.430 ± 0.004	0.48 ± 0.02
Ferrocene/Ferrocinum, Au,0.2 M $KClO_4$ in DMF	8.0×10^{-6}	0.650 ± 0.008	1.44 ± 0.05
$Ru(NH_3)_6^{2+/3+}$, Pt, 3.5 M NH_4Cl, 1.5 M NH_3, in H_2O	8.9×10^{-6}	0.572 ± 0.006	3.9 ± 0.3

[a] Determined from the steady-state limiting current.

to the supporting electrolyte reported rate constants around 0.1−0.2 cm/s for this redox couple.

We also used FR voltammetry to determine the kinetic parameters of ferrocene, $Fe(Cp)_2$, oxidation on a 12.5 μm Au electrode in a DMF solution containing 0.2 M $KClO_4$ and $Ru(NH_3)_6^{3+}$ reduction on a 12.5 μm Pt electrode in aqueous solution containing 1.5 M NH_3 and 5 M NH_4Cl. Results of these measurements are presented in Table 2 and in Figures 11 and 12. Experimental data presented in Figure 11 for $Fe(CN)_6^{3-/4-}$ and $Ru(NH_3)_6^{2+/3+}$ agree very well with the theoretical prediction for $\alpha = 0.43$ or $\alpha = 0.57$ (solid curve), and the results obtained for $Fe(Cp)_2^{0/+}$ are consistent with the theoretical ones for $\alpha = 0.65$ (dashed curve). Faradaic rectification results clearly indicate that electrode processes involving $Ru(NH_3)_6^{2+/3+}$ and $Fe(Cp)_2^{0/+}$ are much faster than the electrode process involving $Fe(CN)_6^{3-/4-}$. The standard rate constants reported in the literature for these systems vary widely (even by orders of magnitude), and it is difficult to select trustworthy results for comparison.

We noted that in aqueous media, FR signals can be obtained even at frequencies exceeding 1 GHz (such results will be described in subsequent papers). On the other hand, conductivity of the DMF solution was much lower than aqueous solutions studied in this work, and in order to achieve a sufficient polarization of the interface, relatively high values of ΔV_{ac} had to be applied (particularly at high frequencies, to compensate for the decreasing ratio of the interfacial impedance to the solution resistance). In DMF, at frequencies above 25 MHz, high values of ΔV_{ac} caused an increase of the dc current in the plateau region of the voltammetric curve (and at the same time, they caused a very significant distortion of the recorded FR curves). These effects can be plausibly explained by the heating of the solution around the microelectrode by high ac currents.[21] Of course, even a small periodic change of the electrode temperature (synchronous with the modulation sequence) makes the FR results invalid. We were vigilant in detecting such cases, and all results reported in this work are free from heating artifacts.

Conclusions

Faradaic rectification voltammetry is experimentally quite simple and it can be carried out with microelectrodes in both aqueous and nonaqueous media. The method is suitable for studies of fast electron transfer reaction. In this work, we proposed a new data analysis that is based only on the shape of FR voltammograms rather than on their magnitude. It has been shown that the kinetic parameters of the electrode reaction can be determined without knowing the interfacial impedance and the solution resistance of the microelectrode. It has to be stressed, however, that our method of data analysis, in its present form, can only be used for simple electron transfer processes that are not accompanied by homogeneous chemical reactions or adsorption of reactants or products.

The method of data analysis used in this work was based on the analytical solution provided by Barker. Unfortunately, this solution is limited to very small amplitudes of the alternating voltage and it is based on the Butler−Volmer formalism.[22] Faradaic rectification measurements are particularly sensitive to changes of the electron transfer coefficient, especially in cases when $\alpha \rightarrow 0.5$. Soon we will present results of numerical simulations of the FR process, with kinetics of electrode processes described in terms of the Marcus theory.[23] Preliminary results indicate that, under the right conditions, there are profound differences between FR voltammograms expected in the case of the Butler−Volmer and Marcus formalisms.

The most important source of errors in FR measurements arises from the possible heating of the electrode in situations when high amplitudes of alternating voltage (ΔV_{ac}) have to be used to overcome ohmic drops. Fortunately, this problem can be resolved by using smaller electrodes. Interfacial impedance of the electrode is inversely proportional to the surface area, and the solution resistance is inversely proportional to the radius of the electrode; therefore, according to eq 8, the ratio $\Delta V_{ac}/\Delta E$ should decrease with a decrease of the electrode radius. With submicrometer electrodes, it should be possible to do reliable FR measurements at GHz frequencies, even in poorly conductive solutions. Such high frequencies may be useful in studies of kinetics of some adsorption processes[24] and in monitoring electron transfer kinetics far from the standard potential.

Acknowledgment. The financial support of the Natural Sciences and Engineering Research Council, Canada (NSERC), through an Individual Discovery Grant is gratefully acknowledged.

References and Notes

(1) Agarwal, H.; Doss, K. *Proc. Indian Acad. Sci.* **1952**, *35A*, 45.
(2) Oldham, K. B. *Trans. Faraday Soc.* **1957**, *53*, 80.
(3) Barker, G.; Faircloth, R.; Gardner, A. *Nature* **1958**, *181*, 247.
(4) Barker, G. C. In *Transactions of the Symposium on Electrode Processes*; Yeager, E., Ed.; Wiley: New York, 1961; p 325.
(5) Delahay, P.; Senda, M.; Weis, C. H. *J. Am. Chem. Soc.* **1961**, *83*, 312.
(6) De Leeuwe, R.; Sluyters-Rehbach, M.; Sluyters, J. H. *Electrochim. Acta* **1967**, *12*, 1593.
(7) Van der Pol, F.; Sluyters-Rehbach, M.; Sluyters, J. H. *J. Electroanal. Chem.* **1973**, *45*, 377.
(8) Agarwal, H. In *Electroanalytical Chemistry*; Bard, A. J., Ed.; Marcel Dekker: New York, 1974; Vol. 7, p 161.
(9) Agarwal, H. P. In Modern Aspects of Electrochemistry; Bockris, J. O'M.; White, R. E.; Conway, B. E., Eds.; Plenum Publishing Corp.: New York, 1989; Vol, 20, p 177.
(10) Sluyters-Rehbach, M.; Sluyters J. H. In *Comprehensive Treaties of Electrochemistry*; Yeager, E. J., Bockris, J. O'M., Conway, B. E., Sarangapani, S., Eds.; Plenum Press: New York, 1984; Vol. 9, p 219.
(11) Galus, Z. *Fundamentals of Electrochemical Analysis*, 2nd ed.; Ellis Horwood: New York, 1994; p 182.
(12) Srinivasan, R.; Murphy, J. C. *J. Electrochem. Soc.* **1991**, *138*, 2960; Erratum: *J. Electrochem. Soc.* **1991**, *138*, 3794.
(13) Grafov, B. M. *Russ. J. Electrochem. (Translation of Elektrokhimiya)* **2003**, *39*, 423.
(14) Franken, P. A.; Hill, A. E.; Peters, C. W.; Weinreich, G. *Phys. Rev. Lett.* **1961**, *7*, 118.
(15) Bard, A. J.; Faulkner, L. R. *Electrochemical Methods*, 2nd ed.; John Wiley: New York; p 643.
(16) Baranski, A. S.; Winkler, K. *J. Electroanal. Chem.* **1998**, *453*, 29.
(17) Bard, A. J.; Faulkner, L. R. *Electrochemical Methods*, 2nd ed.; John Wiley: New York; p 376.

(18) Baranski, A. S.; Szulborska, A. *Electrochim. Acta* **1996**, *41*, 985.
(19) Baranski, A. S.; Krogulec, T.; Nelson, L. J.; Norouzi, P. *Anal. Chem.* **1998**, *70*, 2895.
(20) Huang, W.; McCreery, R. *J. Electroanal. Chem.* **1992**, *326*, 1.
(21) Baranski, A. S. *Anal. Chem.* **2002**, *74*, 1294.
(22) Bard, A. J.; Faulkner, L. R. *Electrochemical Methods*, 2nd ed.; John Wiley: New York; p 92.
(23) Bard, A. J.; Faulkner, L. R. *Electrochemical Methods*, 2nd ed.; John Wiley: New York; p 117.
(24) Baranski, A. S.; Moyana, A. *Langmuir* **1996**, *12*, 3295.